The Depositional Record
The journal of the International Association of Sedimentologists
Open Access

ORIGINAL RESEARCH ARTICLE

Organomineralization processes in freshwater stromatolites: a living example from eastern Patagonia

MURIEL PACTON*,[1], GABRIEL HUNGER†, VINCENT MARTINUZZI†,[2], GABRIELA CUSMINSKY‡, BEATRICE BURDIN§, KURT BARMETTLER¶, CRISOGONO VASCONCELOS* and DANIEL ARIZTEGUI†

*Geological Institute, ETH-Zürich, Zurich, Switzerland
†Department of Earth Sciences, University of Geneva, Geneva, Switzerland
‡Departamento de Ecología CRUB UNC-INIBIOMA CONICET, Quintral 1250, 8400, Bariloche, Argentina
§Centre technologique des microstructures, Université Lyon 1, Lyon, France
¶Institute of Biogeochemistry and Pollutant Dynamics, ETH-Zürich, Zurich, Switzerland

Keywords
Bacterial fossils, biomineralization, extracellular polymeric substances, freshwater microbialite, nanoglobules, stromatolites.

[1]Present address: Laboratoire de Géologie de Lyon, Université Lyon 1, France

[2]Present address: Geneva Petroleum, Geneva, Switzerland

Manuscript received: 22 July 2015; Accepted: 4 January 2016

The Depositional Record 2016; 1(2): 130–146

doi: 10.1002/dep2.7

ABSTRACT

Living stromatolites have been mostly described within shallow marine and (hyper)saline lacustrine environments. Southernmost South America lacks detailed investigations of these (organo)sedimentary buildups, particularly in regions experiencing extreme and variable environmental conditions. Here, we report and describe living freshwater stromatolites in the Maquinchao region, north-western Patagonia, Argentina. Fossil stromatolites characterized by globular and cauliflower shapes are also present in a continuous palaeoshoreline of a former lake at an altitude of 830 m, whereas their living counterparts only occur in the calm waters of sheltered or meandering sections of the Maquinchao River. The living stromatolites and their host waters have been sampled and studied using various chemical and microscopic techniques to better constrain the environmental versus biological factors controlling their development. Our results indicate that today stromatolites only proliferate in freshwater when Ca^{2+} levels are high. A microscopic inspection of the living stromatolite mat indicates stronger photosynthetic activity in the upper green layer associated with crypto/microcrystalline calcite (nanoglobules) compared to the lower beige-white biofilm. This biofilm contains more low-Mg calcite (rhombohedra) precipitates, which can form millimetre-sized aggregates in the underlying anoxic layer. Although sulphate-reducing bacteria are living in the entire mat, they appear more abundant and widely distributed in the lower beige-white layer and are always associated with Mg calcite. Low salinity and low-turbidity water along with microbial (photosynthetic and heterotrophic) activity are the most important factors promoting low-Mg calcite precipitation in the Maquinchao Basin. These conditions are very different from those proposed for recently described lacustrine stromatolites at high altitude in the subtropical and tropical Andes as well as in Chilean Patagonia. Hence, all these observations in modern freshwater stromatolites show the importance of geomicrobiological studies in identifying proxies of the hydrological conditions prevailing during their formation.

INTRODUCTION

Stromatolites constitute some of the oldest evidence for life on Earth (Hofmann *et al.*, 1999). Commonly defined as laminated benthic organosedimentary structures built by the trapping and binding and/or precipitation of minerals via microbial processes (See Riding, 2011), it is no longer clear that all stromatolites represent biogenic structures (Grotzin-

ger & Rothman, 1996; McLoughlin *et al.*, 2008). They can display a variety of morphologies, including columnar, club, spheroidal, domal, nodular or irregular shape (Logan & Cebulski, 1970). The formation of these organosedimentary structures is a consequence of both microbially induced and microbially influenced mineralization (Burne & Moore, 1987; Trichet & Défarge, 1995; Dupraz *et al.*, 2009) in which cyanobacteria are of primary importance.

Due to the variety of surface environments where they occur, their assignment to particular environmental conditions of formation is not always straightforward. Studies of Bahamian stromatolites, for instance, find that lithified interiors beneath surface mat communities are modified by endolithic microbes (Reid *et al.*, 2000). Based on the morphology, marine living stromatolites have been interpreted as analogues of fossil stromatolites. Today, living stromatolites occur in a few shallow marine and mostly (hyper)saline lacustrine environments. In southernmost South America there is a particular scarcity of detailed studies of lacustrine stromatolites in regions subject to extreme and variable environmental conditions. Lately, thrombolites and stromatolites have been identified in Chilean southern Patagonian lakes and used as indicators of palaeoclimate (Solari *et al.*, 2010). To the best of our knowledge, however, no geomicrobiological investigations of the processes governing carbonate precipitation have been conducted. Previous studies on African freshwater stromatolites have shown that they are often distributed along lake shorelines. Thus, they can be used as excellent indicators of hydrological changes in palaeolakes improving the reconstruction of continental palaeoclimates (Casanova & Hillaire-Marcel, 1993). While it is clear that some stromatolites are built in response to microbial forcing (Reid *et al.*, 2000; Awramik & Grey, 2005), results of very recent studies have shown that the frequency of lamina formation is more closely related to regional climate forcing (Andersen *et al.*, 2011; Petryshyn *et al.*, 2012;). Yet, both aspects can be related and even complementary.

Recent freshwater stromatolites from the Maquinchao Basin (north-western Patagonia, Argentina) were studied in order to determine the processes involved in their formation and accretion, while relating these to environmental parameters during their development. Understanding the actual processes governing the formation of these modern microbialites aids in the interpretation of their fossil counterparts formed in the same basin during the last deglaciation and the early Holocene.

STUDY AREA

Laguna Cari-Laufquen is a closed basin (41°8′47″ S, 69°27′37″ W, *ca* 786 m asl; Fig. 1) located in a tectonic depression surrounded by basalt plateaus of Mesozoic to Tertiary age in northern Patagonia, Argentina (Coira, 1979). Presently, the lake system consists of two separate water bodies locally known as Laguna Cari-Laufquen Chica (LCLC; 2·5 × 1·5 km, averaging 3 m water depth in January, 2011), which is a permanent lake body with pH 8·7 (Schwalb *et al.*, 2002) and a sodium bicarbonate concentration of 230 ppm (Galloway *et al.*, 1988); and Laguna Cari-Laufquen Grande (LCLG; 4 × 2 km, average 2 m depth in January, 2011), an ephemeral lake of brackish water with pH 8·8 (Schwalb *et al.*, 2002) and solute concentration of 4000 ppm (Galloway *et al.*, 1988). LCLC sits at 825 m above sea-level, and periodically flows towards the larger basin through the Maquinchao River (Fig. 1). A 20 years series of meteorological data show a mean annual air temperature of 9·0°C ranging from 16·1°C to 1·7°C in Austral

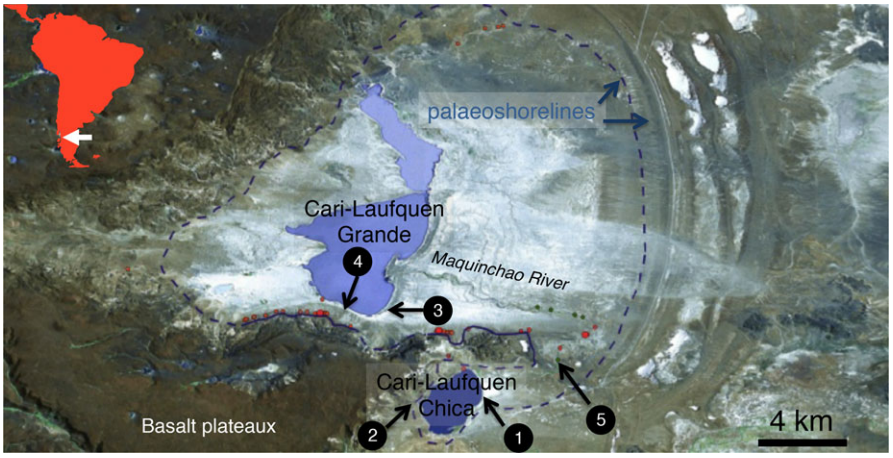

Fig. 1. Satellite image of the Maquinchao Basin (courtesy of GoogleEarth©) showing the location of modern Lagunas Cari-Laufquen Chica and Grande (small and large, respectively). Red and green dots indicate fossil and living stromatolite occurrence, respectively. Numbered black dots indicate sampling sites (see text), whereas blue arrows show palaeoshorelines.

summer and winter seasons, respectively, whereas annual precipitation averages 31·6 cm over the same time interval (source: Argentinean Meteorological Survey). Previous investigations have shown evidence of former lake-level high stands during which both lakes LCLG and LCLC were merged to form a large palaeolake in the late Pleistocene (Del Valle *et al.*, 1993, 1996). This lake encompassed more than 1500 km^2 and was at least 70 m deep during the pluvial phase maximum (González Bonorino & Rabassa, 1973; Volkheimer, 1973; Coira, 1979; Galloway *et al.*, 1988; Tatur *et al.*, 2000; Ariztegui *et al.*, 2008). Several palaeoshorelines indicate higher lake levels than today (Fig. 1). They have been previously dated at *ca* 19 ka (Galloway *et al.*, 1988) and between 14 ka and 10-8 ka BP (Bradbury *et al.*, 2001). Furthermore, lacustrine sediments outcropping within the Maquinchao Basin document a well-defined Late Pleistocene pluvial episode (Whatley & Cuminsky, 1999; Cusminsky *et al.*, 2011) followed by a prograding sedimentary sequence. Stromatolites, also called 'tufa' by Cartwright *et al.* (2011), are widely distributed in the Laguna Cari-Laufquen often tracing the palaeoshorelines. They display a variable structure ranging from cauliflower to more globular with a nucleus of various compositions depending on their location. Fossil stromatolites showing a globular aspect can form plurimetric complexes and are present in a continuous palaeoshoreline at an altitude of 830 m (Figs 1, 2A and 3), dated at *ca* 22·0 ka BP (Cartwright *et al.*, 2011). Globular carbonate laminated structures most commonly surround a basaltic nucleus and do not exhibit any growth preferential axis or other evidence of hydrodynamic conditions.

MATERIALS AND METHODS

Samples

Growing microbial bodies showing a globular structure similar to fossil stromatolites have been found in the Maquinchao River and are the subject of this study (Figs 2B and 4). Five living stromatolites attached to their substrate (basaltic pebbles) were sampled in the field in January, 2011 (Austral summer) when they were subaerially exposed, preserved in sterile 50-ml plastic tubes and stored at 4°C. The biofilms were subsampled by manual separation into a *ca* 1 mm thick surface sample (green biofilm) and an underlying sample taken from *ca* 2 to 3 mm below the surface (beige-white biofilm). Each layer was observed by optical microscopy under natural light (with prior ultrasonic for 30 sec) and air-dehydrated for scanning electron microscopy (SEM), while the entire stromatolite mat was observed using confocal laser scanning microscopy (CLSM).

Surface water samples were taken in five distinct areas as follows (Fig. 1): (1) The LCLC outflow towards the Maquinchao River; (2) LCLC shore area; (3) LCLG shore area; (4) groundwater stream close to a vegetated area on the LCLG shore; and (5) sheltered section of the Maquinchao River containing living stromatolites. Today, the maximum 3 m depth of both lakes results in a water column which is continuously mixed making sampling at different depths unnecessary. Physicochemical data, that is, temperature, pH, salinity and conductivity were measured at all sites before sampling (Fig. 3A and B).

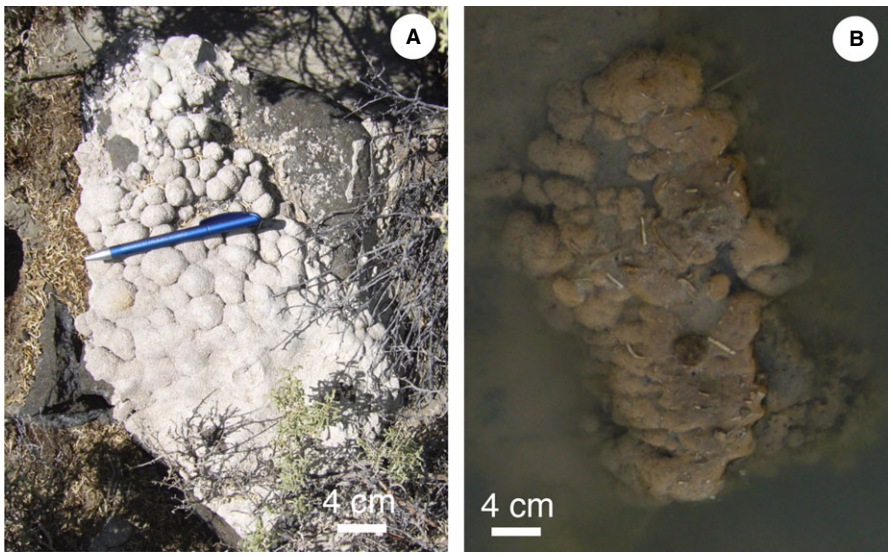

Fig. 2. Photograph of fossil globular stromatolite dated around 22 Ka BP (A); and partially submerged living globular stromatolites growing in a sheltered area beneath calm waters in the Maquinchao River (B).

Fig. 3. Outcrops showing fossil globular stromatolites along a palaeoshoreline.

Methods

Twenty millilitre of each water sample was filtered (0·2 μm nylon filters) and acidified (1% v/v concentrated HCl) for subsequent elemental analysis by inductively coupled plasma – optical emission spectrometry (ICP-OES, Varian Vista MPX, ETH Zürich). The extraction was performed on two to four independently incubated samples.

Water samples were analysed for their stable isotope composition (δD and $\delta^{18}O$, referenced to Vienna Standard Mean Ocean Water (VSMOW) at the Alfred Wegener Institute for Marine and Polar Research (AWI) Potsdam, Germany. A Finnigan MAT Delta-S mass spectrometer equipped with two equilibration units was used for the online determination of hydrogen and oxygen isotopic compositions. The external errors for standard measurements of hydrogen and oxygen are better than 0·8‰ and 0·1‰, respectively (Meyer *et al.*, 2000).

Various microscopic techniques were used to analyse the stromatolite structure down to the nanoscale: optical microscopy (Axioscope, ETH Zürich) under transmitted light, CLSM (Centre Technologique des Microstructures, Université Lyon 1, France), SEM (Jeol Zeiss Supra 50 VP, University of Zurich) on platinum coated samples prior to fixation with glutaraldehyde, and transmission electron microscopy (TEM, Phillips CM100, Centre Technologique des Microstructures, Université Lyon 1, France) after staining sectioned samples (Amann *et al.*, 1995). Investigation of stained samples and control materials was carried out using a Zeiss LSM 510 META. Staining procedures for fluorescence *in situ* hybridization (FISH) were modified from Decho & Kawaguchi (1999). Samples were stained with the 16S rRNA probe SRB385 (CGGCGTCGCTGCGTCAGG) labelled with cyanine 3 to image sulphate-reducing bacteria (SRB). This oligoprobe targets SRB of the **y**-proteobacteria (Amann *et al.*, 1990). Photosynthetic organisms and carbonate minerals were visualized by fluorescence. Unstained green biofilms were excited by the 633 nm laser line with the fluorescence detected above 650 nm, while the unstained beige/white biofilms were excited by the 543 nm laser line with fluorescence detected using a 560 nm long pass filter. Both biofilms were excited by a different wavelength in order to distinguish the autofluorescence of ostracods from that of cyanobacteria in the green biofilm. Autofluorescence from filamentous cyanobacteria in the unstained biofilms has been spectrally separated from the red-shifted autofluorescent calcite and indicated by the development of an artificial green colour. The Cy3-labelled probe SRB385 was excited by the 488 nm laser line with the fluorescence detected between 500 and 555 nm. CLSM Image analyses were performed using Image J and Imaris software version 5·6.

Samples from fossil and living stromatolites were ground to an ultrafine powder in an agate mortar before being placed in a silicon wafer and a plastic sample holder for X-Ray diffraction analyses (XRD). They were

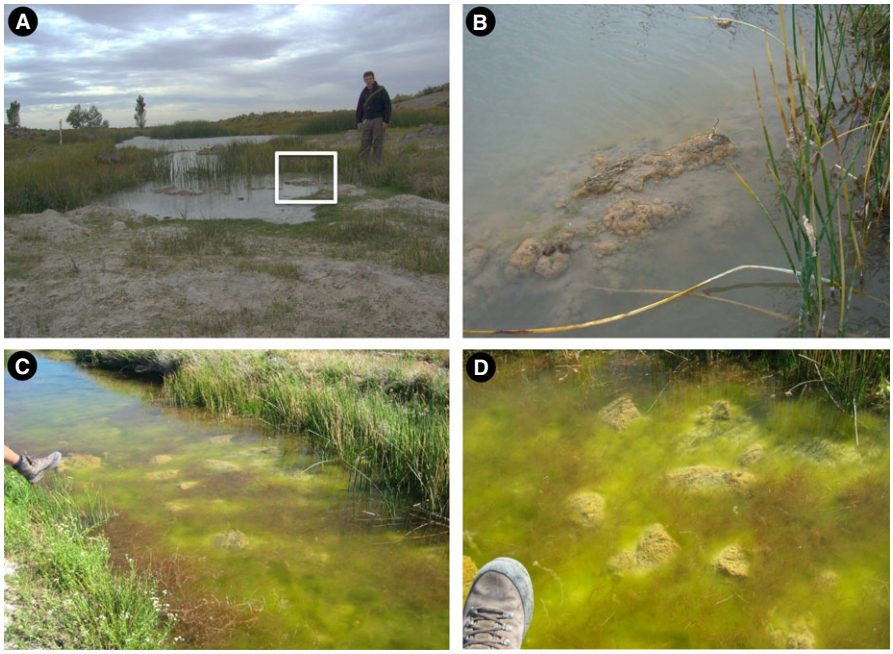

Fig. 4. Location of the living stromatolites in the Maquinchao River: (A) meander-like area; (B) details of (A); (C and D) abundant green slime between stromatolites.

analysed in a Bruker, AXS D8 Advance device, equipped with a Lynx-eye super-speed detector using Cu-K radiation and an anti-scattering slit of 20 mm, while rotating the sample. The sample patterns were recorded from 5° to 85° 2θ in steps of 0·004°, 1 sec counting time per step.

RESULTS

Water chemistry

The water chemistry of LCLG and LCLC, as well as that of the Maquinchao River varies by location. January, 2011 (Austral summer) was particularly hot and dry and the Maquinchao River was partially cut from LCLC being almost entirely fed by groundwater while flowing towards LCLG. This situation implies differential evaporation between the two lakes and the river (e.g. LCLC was almost dry) and consequently supports their different chemistry. Both shore and outflow water of LCLC display temperatures above 33°C while they are around 27°C at the other sites (3, 4 and 5; Fig. 5A). The pH in the water column ranged from 8·1 (where stromatolites are living and in the Maquinchao River) to 9–9·4 in both lakes. Salinity was fairly constant in most of the sampled sites indicating brackish conditions (1·3–12·5‰). However, the riverine waters in which stromatolites are presently growing display more freshwater conditions (0·7‰).

Major and minor ions show some differences between the lakes and the other sites. Waters are dominated by Na with concentrations ranging from 150 up to 4750 ppm, while Ca and Mg concentrations average 19 and 68 ppm, respectively. For cations, the major elemental abundances in both lakes were $Na^+ \gg Mg^{2+} > K^+ > Ca^{2+} > Si^{4+}$, whereas the relative abundances were $Na^+ \gg Ca^{2+} > Mg^{2+} > K^+ > Si^{4+}$ at the other sites (Table 1; Fig. 5B). Sulphur displays similar concentrations to Na and is likely present as SO_4^{2-} (Schwalb *et al.*, 2002). The Mg concentration was as high as 100 ppm and 200 ppm in LCLG and LCLC, respectively, whereas it was less than 25 ppm at the other sites. The highest Ca concentration (42 ppm) was measured where stromatolites are presently living, while minimum values were found in both lakes (around 7 ppm). Silicon concentrations of 3 or 4 ppm in both lakes contrasted with values reaching 20 ppm in the river and groundwater. The Mg:Ca ratio is typically greater than 15 and 25 in both lakes, whereas the other sites display ratios lower than 1.

Figure 6 shows that LCLG and LCLC samples are characterized by ^{18}O-enriched waters (9·53 and 5·82‰), whereas the groundwater and Maquinchao River sites display depleted values (−10‰ and −87‰ for $\delta^{18}O$ and δD, respectively). Lake waters are enriched isotopically compared to those reported by Schwalb *et al.* (2002) and Cartwright *et al.* (2011) which is consistent with the comparatively lower water levels of our sampling year. How-

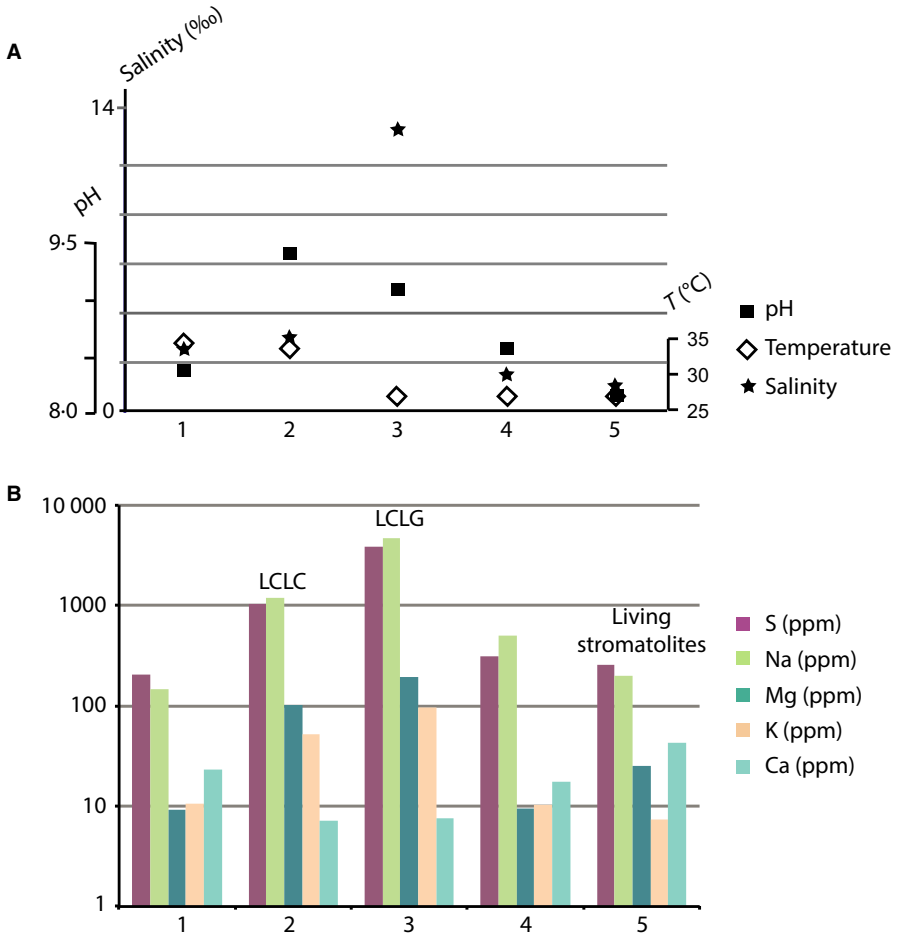

Fig. 5. (A): Temperature, pH and salinity of the sites sampled in January, 2011 (Austral summer). Refer to Figure 1 for sample location. (B) Stacked column plot showing the relative variation in main ions (ppm) for the individual sampled sites (log scale).

ever, the lake waters as a whole form a well-defined δD-$\delta^{18}O$ mixing line with river-supplied inflow (Craig *et al.*, 1974). This line is geometrically coincident with and statistically identical to a regression line computed from the lake data alone ($r = 0{\cdot}97$), indicating that lake waters evolved from the same primary water sources. Groundwater and Maquinchao River waters plot along the global meteoric water line, implying very low to non-evaporation. Despite the lack of *in situ* physicochemical measurements throughout the year, the existing meteorological data for the area suggest contrasting seasonal changes. It appears, however, that the biota is adapting to these conditions through time.

Living stromatolites sample description

Five stromatolite samples were collected from the Maquinchao River during mid-January 2011. Living stromatolites are found in several protected areas of the river such as the quiet water of meanders (Fig. 4A). Waters are less turbid here than in either of the lakes and contain abundant green slime between the stromatolites (Fig. 4B–D). These carbonate buildups display a globular morphology (Fig. 7) with a thin (*ca* 1 mm thick) outermost biofilm composed of a green layer overlying an undulating beige-white layer, varying in thickness between 4 and 9 mm (Fig. 4B–D).

A series of XRD analyses in both the green and beige-white layers showed that low-Mg calcite is the main mineral phase (70%) with a few detrital quartz grains and halite, which is an artefact of the sample processing. No crystalline Mg-Si minerals have been found. Similarly, low-Mg calcite is the dominant mineral phase in the fossil stromatolites displaying a Mg/Ca ratio of about 0·03.

Upper green layer of the stromatolite mat

The green layer is composed of mainly filamentous and coccoid bacteria (Fig. 8A) with little granular amorphous organic matter (OM) (white arrow in Fig. 8A). These

Table 1. Chemical characteristics of water samples. Refer to Fig. 1 for sample location

Samples	Ca (ppm)	K (ppm)	Mg (ppm)	Na (ppm)	S (ppm)	Si (ppm)	Al (ppm)	Ni (ppm)	As (ppm)	Ba (ppm)	Cu (ppm)	Fe (ppm)	P (ppm)	Zn (ppm)
1	23·2459	10·6006	9·3463	144·83	207·555	0·9659	0·012	0·002	0·0892	0·05335	0·00045	0·0348	0·3391	0·00215
2	7·0766	51·7111	103·115	1200·81	1029·72	4·8983	0	0·0068	0·1671	0·04355	0·0096	0·00605	1·1572	0·00355
3	7·4915	96·195	194·3125	4750·85	3836·9	3·35175	0	0·0037	0·3354	0·04865	0·00445	0·00335	0·1043	0·0012
4	17·3791	10·2204	9·58155	508·265	315·04	20·05	0·0011	0·0014	0·1639	0·02355	0·0017	0·005	0·753	0·01525
5	42·4272	7·3061	25·5225	198·19	259·775	12·91845	0·0061	0·0066	0·07755	0·01835	0·0014	0·0011	0·0308	0·00425

bacteria are mostly photosynthetic as shown by their green colour under natural light and red autofluorescent pigments due to chlorophyll and phycobiliproteins (Fig. 8A and C), in addition to the presence of *Spirulina* (data not shown). Their abundance is supported by the strong autofluorescence in the first millimetre of the mat compared to the deeper layers (Fig. 8C). Microcrystalline low-Mg calcite is widely observed associated with cyanobacteria as characterized by the mixed, that is, yellow colour. The blue-fluorescing SRB are co-localized with the red-fluorescing cyanobacteria indicating that SRB are living in oxic conditions (Fig. 8E). Microbial communities are trapped with diatoms within an extracellular polymeric substances (EPS) matrix (Fig. 9A). Diatoms are partially to entirely dissolved (Fig. 9B) when completely trapped by EPS. Organic filaments (Fig. 9C) and cryptocrystalline low-Mg calcite are embedded within EPS. Mineralized EPS are Ca-enriched (Fig. 9D) compared to low-Mg calcite (Fig. 9E). The latter is always associated with low Si content (from likely dissolved diatoms), while no Al was detected (Fig. 9E). Micro/cryptocrystalline low-Mg calcites are either characterized by nanoglobules (Fig. 9F) or arranged as platelets, closely associated with EPS suggesting an *in situ* growth. This low-Mg calcite crystal arrangement creates a nanoporosity (Fig. 9F). Examination by TEM confirms that this biofilm is mainly composed of cyanobacteria as shown by multiple rows of tightly stacked thylakoids, that is, membranes where photosynthesis occurs (Fig. 10A), indicating healthy, active photoautotrophic organisms (Stolz, 1991). Extracellular polymeric substances were distributed as nanofilaments creating a mesh-like network that is not restricted to the surface of the cells (Fig. 10B). Other microorganisms such as rod-shaped Gram-negative bacteria have also been identified (Fig. 10C), probably SRB.

Lower beige-white layer of the stromatolite mat

The beige-white biofilm displays more granular amorphous organic matter (AOM) compared to the green biofilm (Fig. 8B) and an association of coccoid cyanobacteria and colourless dead filaments (Fig. 8B). Some filaments were also photosynthetic as shown by their red autofluorescence (Fig. 8D) but most were colourless in contrast to the green colour they displayed in the overlying biofilm. Green, autofluorescent, low-Mg calcite crystals occur locally in conjunction with cyanobacteria (Fig. 8D) but are more abundant when associated with SRB (Fig. 8F) in this layer than they are in the overlying green one. Extracellular polymeric substances and microcrystalline low-Mg calcite form a complex matrix (Fig. 11A and B). These crystals occur as stacks of platelets which combine further to form rhom-

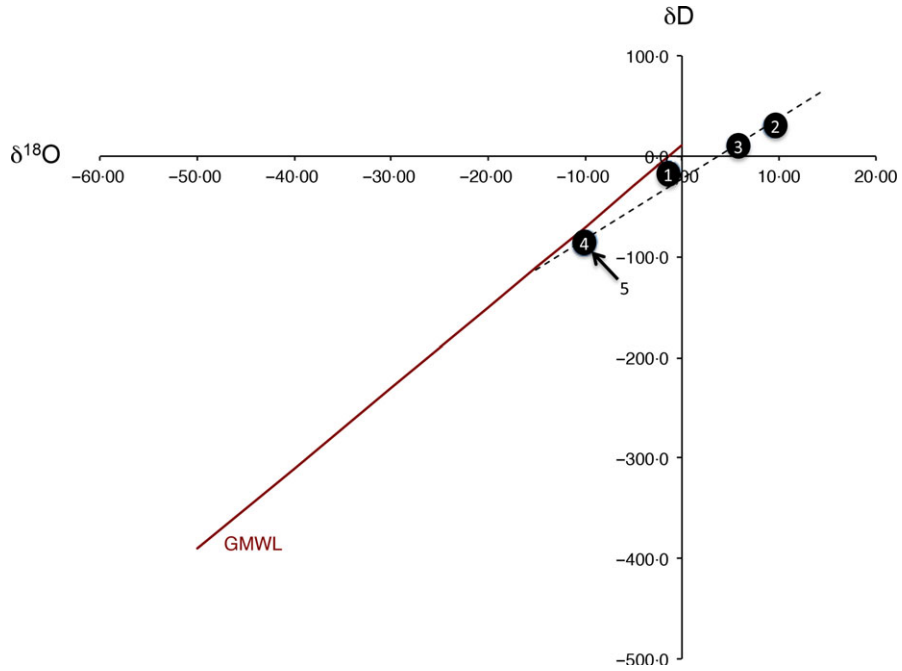

Fig. 6. Variations in δD versus $\delta^{18}O$ of water samples (refer to Fig. 1 and text for location). Global meteoric water line (GMWL) from Craig & Gordon (1965).

bohedra (Fig. 11F). The surface of the platelets is characterized by a nanoglobular structure (Fig. 11C) connected by nanofilaments of EPS (Fig. 11C). These crystals, consisting of low-Mg calcite, were associated with a small amount of silicon possibly resulting from diatom dissolution (Fig. 11D). The ultrastructure of this biofilm consists primarily of dying cyanobacteria surrounded by substantial fibrillar EPS (Fig. 10D) together with the remains of partially dissolved diatoms. Large quantities of fibrillar EPS can form aggregates containing several cells (Fig. 10D). The abundance of empty cyanobacterial sheathes along with the increased density of the collapsed sheath material are indicative of dying cyanobacteria (Fig. 10E) and indicate early to advanced stages of degradation (Stolz *et al.*, 2001). Ample virus-like particles have been found, sometimes icosahedral in shape (Pacton *et al.*, 2014; Fig. 10F).

DISCUSSION

Environmental conditions constraining stromatolite occurrence in the Maquinchao Basin: implications for palaeohydrological reconstructions

Clear differences in water composition have been observed between the presently growing stromatolites and the other sampled sites. These differences allow the environmental parameters controlling stromatolite growth to be identified and, thus, permit the conditions of carbonate precipitation in their fossil counterparts to be estimated. Firstly, the alkaline pH throughout the different sampling sites, that is, 8·1–9·4, indicates that this parameter is not a determining factor for the presence of stromatolites. Secondly, the living stromatolites appear to prefer freshwater rather than the more turbid and brackish lake waters. Thirdly, calcium is the most significant element in the freshwater sites, contrasting with the brackish waters of both present-day lakes where Mg and K dominate (Fig. 5B). Similarly to the high-altitude volcanic lakes of Patagonia, the water of both lakes contains essentially all inorganic nutrients, and at much higher concentrations (except for Ca), than the Maquinchao River, making it unlikely that the input of these chemicals is critical for stromatolite development (Farias *et al.*, 2013). Although nutrient availability has not been investigated in detail, turbidity is one of the most important factors constraining stromatolite development in the Maquinchao Basin. It is widely accepted that the presence of dissolved Mg^{2+} inhibits the precipitation of calcite favouring the precipitation of aragonite, especially with a Mg^{2+}:Ca^{2+} ratio >12 (Bischoff & Fyfe, 1968; Müller *et al.*, 1972; Berner, 1975). Therefore, the palaeolake in which the fossil stromatolites were living most probably had a lower Mg^{2+}:Ca^{2+} ratio than today and was thus closer in composition to the Maquinchao River.

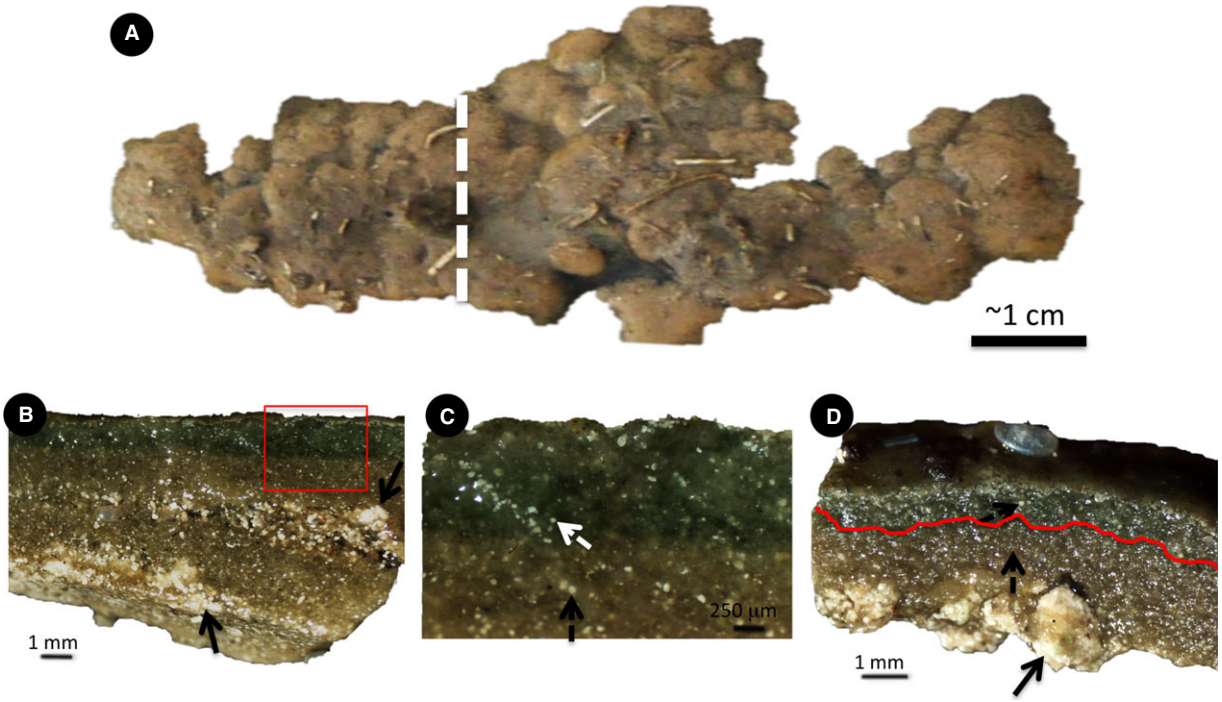

Fig. 7. Top view (A) and cross-section of a recent globular stromatolite mat (dashed line). Note the carbonate concretions in the beige/white layers (arrows).

At present, the Maquinchao region is one of the driest in the world but both lake basins show geomorphological evidence (palaeo-shorelines) of major fluctuations in the water balance since the last deglaciation. According to Bradbury *et al.* (2001) the large Cari-Laufquen palaeolake experienced several high stands during the Late Pleistocene and Early Holocene. These lacustrine basins had low productivity and were less saline and turbid than today. Lakes fed by rivers draining volcanic terrains of dominantly basic composition, coupled with groundwater inflow could create a set of conditions involving high CO_2 input and carbonate alkalinity, high dissolved silica, and high levels of Mg, Ca and Na (Wright, 2012). According to Valero-Garcés *et al.* (2001) Quaternary lacustrine travertines and stromatolites from high-altitude Andean lakes in north-western Argentina were probably formed during low lake levels, when conditions were more favourable for cyanobacterial growth than for plant development. These authors suggested that grazing of microbial mats could be another factor preventing stromatolite formation as microbial mats form the basis of benthic food webs that include metazoan consumers such as gastropods, microcrustaceans, insect larvae and vertebrates (Elser *et al.*, 2005). The geochemical and microscopic studies of the Cari-Laufquen stromatolites presented here clearly indicate that, in the Maquinchao Basin, stromatolites only proliferate under dominantly freshwater conditions corresponding to meander-like fluviatile environments. Although the effect of seasonal variations on stromatolite development has yet to be studied, cold periods might reduce microbial metabolic activity and subsequent carbonate precipitation (Plée *et al.*, 2008). Thus, living stromatolite mats provide a proxy to reconstruct the prevailing environmental conditions influencing growth of their fossil counterparts in the same basin. These results agree with the presence of fossil stromatolites along the late Pleistocene palaeoshorelines.

Stromatolites: the role of microbial communities in carbonate precipitation

There are several significant differences in macroscopic characteristics and species composition between the two biofilm layers constituting the stromatolites. Firstly, both the green and beige/white biofilms contain filamentous and coccoid cyanobacteria, diatoms and other heterotrophs, but in different relative abundances. We observed an increase in dead photosynthetic microbes in the underlying beige/white biofilm as shown by their colourless aspect (Grilli Caiola *et al.*, 1993) along with an increase in SRB and other heterotrophs. Examination by TEM of the beige/white biofilm confirms the increased

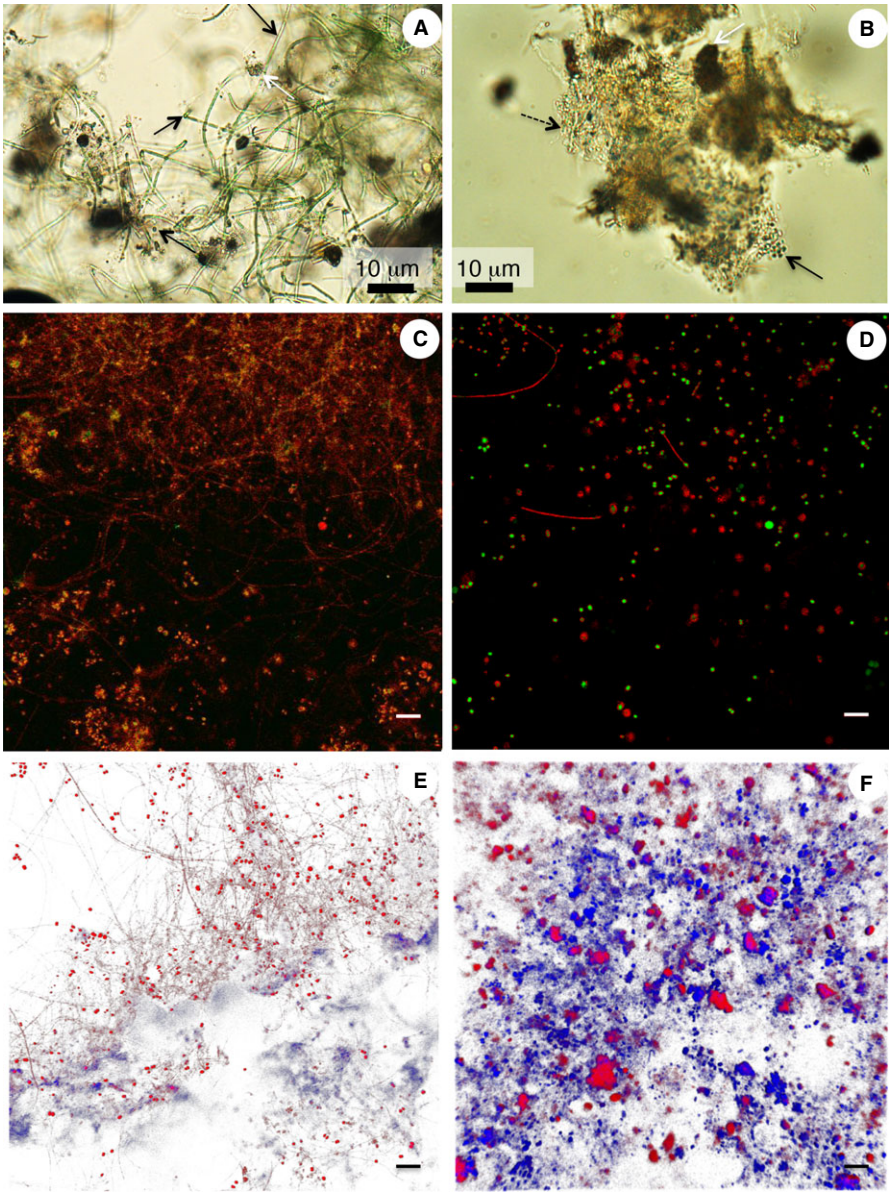

Fig. 8. Recent globular stromatolite mat (A) Light micrographs of the green biofilm showing photosynthetic cyanobacteria (black arrows) and translucent filamentous bacteria (dashed black arrow) associated with amorphous organic matter (AOM, white arrow); Light micrographs of the beige/white biofilm showing coccoid cyanobacteria (black arrow) and translucent dead filamentous bacteria (dashed black arrow); granular AOM (white arrow); (C and D) False colour confocal scanning laser microscopy (CSLM) cross-sectional image of the stromatolite mat showing abundant cyanobacteria (red) in the upper green biofilm and more abundant calcite crystals (green) in the beige/white biofilm (D); (E) some clusters of sulphate-reducing bacteria (SRB, blue) associated with filamentous cyanobacteria and calcite crystals (red autofluorescence) in the green biofilm; (F) Abundant SRB associated with calcite crystals (red autofluorescence) in the beige/white biofilm (F). SRB are detected using a fluorescence *in situ* hybridization (FISH) oligoprobe (SRB 385).

degradation of cyanobacterial cells as well as degradation of EPS into fine fibres. The latter is associated with an increase in granular AOM suggesting OM degradation of microbial origin (Pacton *et al.*, 2011). This associattion might be due to the aerobic respiration and/or sulphate reduction of microorganisms. Such SRB are known not only to survive oxic conditions but also to thrive in the presence of cyanobacteria (Canfield & Des Marais, 1991; Dupraz & Visscher, 2005; Baumgartner *et al.*, 2006) resulting in the partial degradation of EPS and low molecular weight organic carbon (LMW-OC) (Decho, 2000; Glunk *et al.*, 2011). Virus-like particles have also

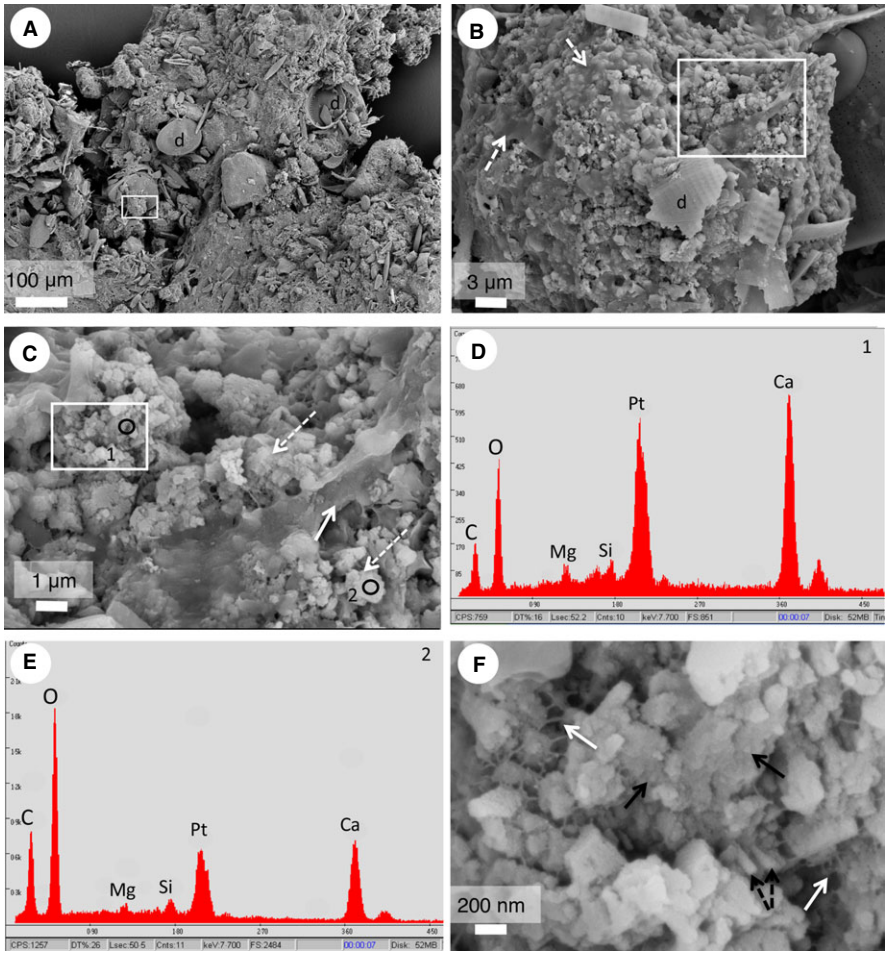

Fig. 9. Scanning electron microscope images of the green biofilm: (A) the biofilm contains different diatom morphospecies (d) which are embedded in an organo-mineral matrix (see boxed area enlarged in B); (B) this organo-mineral matrix is composed of EPS (dashed arrows) and partially dissolved diatoms (d); (boxed area enlarged in (C); (C) EPS (white arrow) are closely associated with single low-Mg calcite crystals (white dashed arrows) and fluffy minerals and enlarged in E (black circles represent spot for EDS analysis in D and E); (D) Elemental analysis showing low-Mg calcite and EPS associated with Si; (E) Elemental analysis of LMC showing a small contribution of Si; (F) Mineralized nanoglobules (black arrows) and platelets (dashed black arrows) closely associated with EPS (white arrows). Nanoporosity characterized by an alveolar network, that is, EPS.

been identified in both biofilms, free within EPS, but appeared more abundant in the beige/white biofilm. It is known that viruses are the most abundant biological entities throughout marine and terrestrial ecosystems (Suttle, 2005), and more specifically in modern microbial mats (Desnues *et al.*, 2008; Pacton *et al.*, 2014). As they have been found in the biofilm associated with degraded cells, we suggest that they may have been involved in the infection of these cells. It is known that viruses represent the largest fraction of nanosized particles that can undergo degradation or, under specific conditions, mineralization processes (Pacton *et al.*, 2014). Viruses have been found as important mineralized entities in microbial mats (Pacton *et al.*, 2014; De Wit *et al.*, 2015) although an alternative origin such as membrane vesicles (MVs) cannot be ruled out. The latter share morphological and chemical similarities and could outnumber viral particles in sea water samples, especially when they are quantified using epifluorescence microscopy (Forterre *et al.*, 2013; Biller *et al.*, 2014). However, according to Soler *et al.* (2015), the abundance of MVs could also be overestimated as they could contain viral genomes. Further studies are required to better discriminate MVs from true viruses in environmental samples.

Although there is no mineralogical difference between the carbonates of both biofilm layers (low-Mg calcite), crystal morphologies are quite distinctive. Low-Mg calcite crystals in the outermost green biofilm are either characterized by nanoglobules (probably mineralized viruses) or arranged as platelets associated with Si and EPS. The

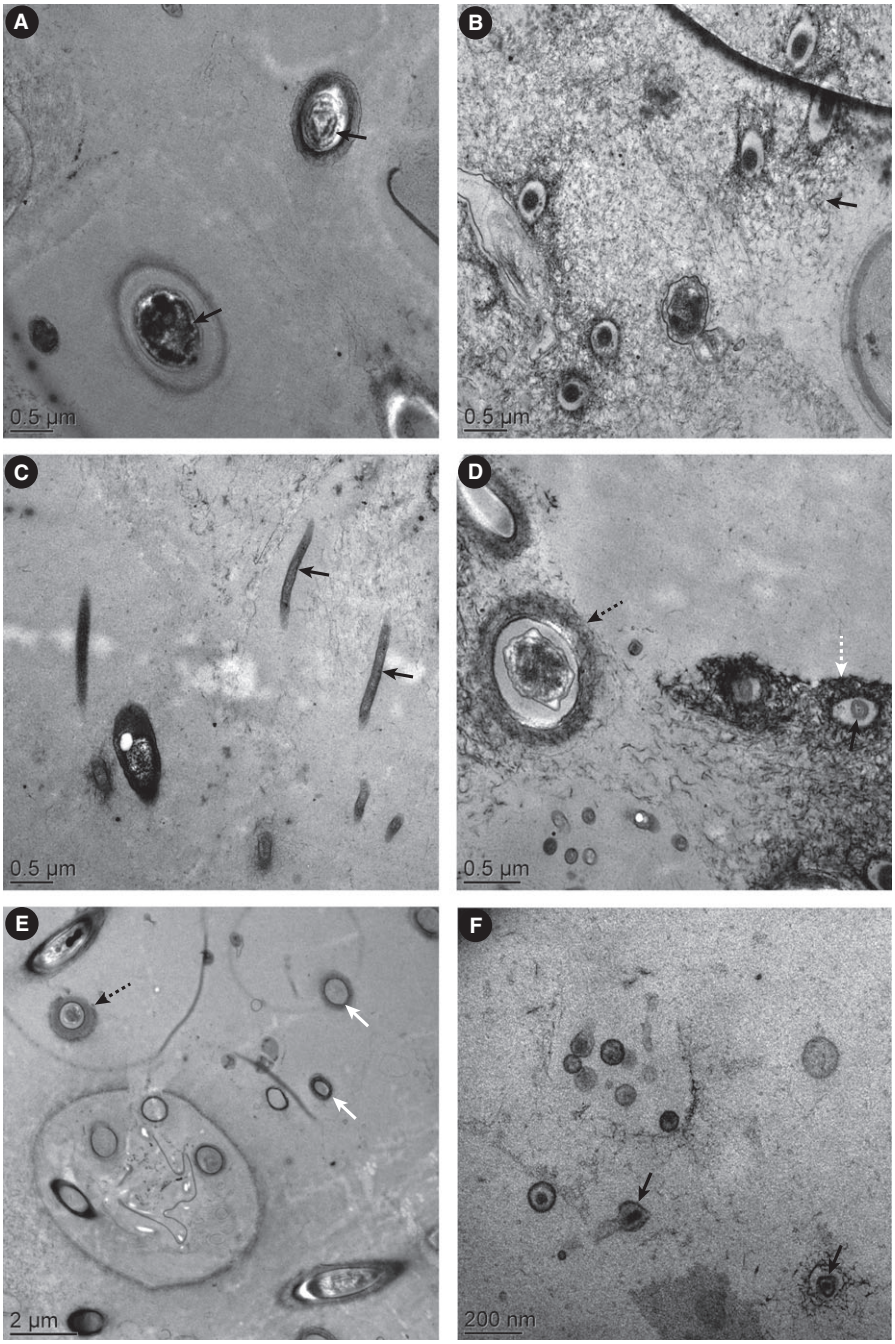

Fig. 10. Transmission electron microscope images of the green (A–C) and beige/white (D–F) biofilms: (A) filaments of cyanobacteria enclosed in their sheath in cross-section with thylakoid membranes (arrows); (B) EPS appear as nanofilaments creating a mesh-like network through the layer and are not restricted to the surface of the cells (arrow); (C) several rod-shape Gram-negative bacteria (arrows); (D) Dying cyanobacteria (black arrow) are surrounded by substantial fibrillar EPS (dashed black arrow) and comprise several cells together (dashed white arrow); (E) thick sheath surrounding cyanobacterial cells in the early stages of degradation (dash arrow) and abundant empty cyanobacterial sheaths in the advanced stages of degradation (white arrows); (F) abundant virus-like particles showing sometimes icosahedral shape (black arrows).

platelets within the beige/white biofilm tend to form euhedral rhombohedra that are often coated or partially filling the pore spaces of the biofilm. The EPS show an enrichment in Si-Ca-Mg elements suggesting that they are mineralized as amorphous Mg-Si ($_{am}$Mg-Si) phases associated with low-Mg calcite (Fig. 11D).

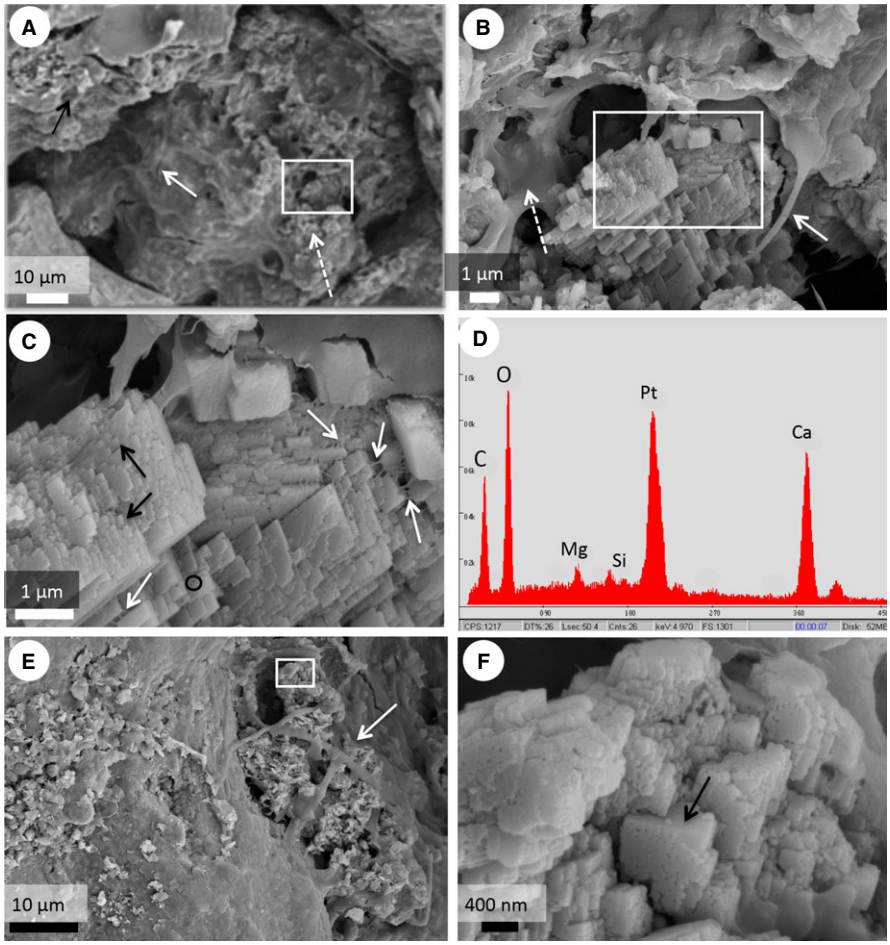

Fig. 11. Scanning electron microscope images of the beige/white biofilm: (A) the biofilm contains thick EPS layers (white arrow) or occurs as an alveolar network (boxed area enlarged in B), which are closely associated with mineral precipitates (dashed arrow); (B): EPS can be filamentous (arrow) or as a thin veil (dashed arrow) associated with low-Mg calcite crystals as oriented platelets (boxed area enlarged in (C); (C) EPS surround platelets (white arrows), which show nanoglobules at surface (black arrows) and the typical 2D orientation suggests a rhombohedra precursor; (D) Elemental analysis of platelets indicates low-Mg calcite. The small amount of Si can be related to surrounding EPS; (E) Single crystals embedded in EPS and enlarged in F; (F) euhedral rhombohedra (black arrow).

Amorphous Mg-Si precipitates have previously been reported in numerous environments, always associated with microbial activity (Arp *et al.*, 2003; Souza-Egipsy *et al.*, 2005; Benzerara *et al.*, 2010; Pacton *et al.*, 2012). It has also been demonstrated that $_{am}$Mg-Si enhances fossilization of microbes, and is commonly found in the rock record. The authigenesis of $_{am}$Mg-Si phases is, however, poorly understood, with previous work suggesting that $_{am}$Mg-Si layers in microbialites replace a primary mineral phase (Arp *et al.*, 2003). In contrast, this data favour a primary origin for these $_{am}$Mg-Si phases. The close association between carbonate crystals, EPS and $_{am}$Mg-Si suggests that the precipitation is microbially mediated. The microbially mediated precipitation pathways are called organomineralization processes and are defined as (i) biologically induced mineralization resulting from the interaction between biological activity and the environment; and (ii) biologically influenced mineralization, which is a passive mineralization of organic matter (biogenic or abiogenic in origin), influencing crystal morphology and composition (Dupraz *et al.*, 2009).

In the green biofilm, most of the mineral phases appear as a complex of Mg-Si and Ca characterized by nanoglobules closely related to EPS. Initially the negatively charged functional groups in fresh EPS bind Ca^{2+} and Mg^{2+}, inhibiting carbonate precipitation (Dupraz *et al.*, 2009). Nanoglobules of EPS could be the first step towards mineralization as EPS have been reported to be permineralized as amorphous Mg-Si phases ($_{am}$Mg-Si) before being calcified (Souza-Egipsy *et al.*, 2005; Pacton *et al.*, 2012).

In the underlying beige/white layer, sulphate reduction and possible respiration would increase availability of Ca^{2+}, promoting carbonate precipitation as rhombohedra (Dupraz & Visscher, 2005). The EPS act as a template for carbonate precipitation arranging platelets into rhombohedra suggesting an EPS-influenced organomineralization. As SRB have been shown to be highly active in lithified zones of microbial mats (Visscher *et al.*, 2000; Dupraz *et al.*, 2004), they might have been involved in lithification of stromatolites. However, SRB and other heterotrophs could have reduced EPS by breaking down exopolymers and inhibiting precipitation in the upper green layer (Arp *et al.*, 2012). This phenomenon is illustrated by the degradation of nanofilaments of EPS into fine fibres. Further investigation of the fossil stromatolites is required in order to decipher the biotic from the abiotic contribution to their formation.

Although cyanobacteria primarily contribute to stromatolite morphogenesis, the metabolic activity of heterotrophic bacteria such as SRB is also significant in microbial mats (Canfield & Des Marais, 1991; Visscher *et al.*, 2000; Des Marais, 2003; Dupraz *et al.*, 2004). The globular morphology of these stromatolites likely reflects specific microbial responses to their environment, which may result from differential growth, migration of microbes with respect to environmental conditions such as light, O_2, etc. or a combination of both (Andersen *et al.*, 2011).

CONCLUSIONS

Modern stromatolites from the Maquinchao Basin (Argentina) are presently formed by microbial communities including filamentous and coccoid cyanobacteria, non-photosynthetic microorganisms capable of respiration and/or sulphate reduction, and diatoms. Combining water chemistry and microscopy data enabled the optimum conditions for stromatolite growth to be constrained.

Unlike recently described stromatolites at high altitude in the subtropical and tropical Andes, a combination of low salinity and turbidity, relatively high Ca and microbial (photosynthetic and heterotrophic) activity appear to be some of the most important factors promoting low-Mg calcite formation in the Maquinchao Basin. Our results further indicate that carbonate formation is mediated by organomineralization processes in which EPS play a fundamental role. Freshwater stromatolites appear to be a useful proxy for changing hydrological conditions. They also highlight the significant role of modern geomicrobiological studies in understanding the mechanisms and environmental conditions underlying their formation.

ACKNOWLEDGMENTS

Fieldwork was accomplished with the generous funding of the *Fondation Augustin Lombard*, Geneva (Switzerland) to G. Hunger and V. Martinuzzi, the logistic support of the Argentinean Research Council (CONICET PIP 00819) National Agency for the Promotion of Science and Technology (PICT 2010-0082), and the University of Comahue (Grant B166) Bariloche, Argentina. We thank the University of Geneva, ETH-Zürich, the Swiss National Science Foundation (grant 2000.112320), and Pethros (Petrobras) for financial support, and the University of Zurich for access to SEM facilities. We also acknowledge Hanno Meyer for isotopic water measurements and Genort Arp for helpful comments on an earlier version of the manuscript.

References

Amann, R.I., Binder, B.J., Olsen, R.J., Chisholm, S.W., Devereux, R. and **Stahl, D.A.** (1990) Combination of 16S rRNA-targeted oligonucleotide probes with flow cytometry for analyzing mixed microbial populations. *Appl. Environ. Microbiol.*, **56**, 1919–1925.

Amann, R.I., Ludwig, W. and **Schleifer, K.** (1995) Phylogenetic identification and in situ detection of individual microbial cells without cultivation. *Microbiol. Rev.*, **59**, 143–169.

Andersen, D.T., Sumner, D.Y., Hawes, I., Webster-Brown, J. and **McKay, P.C.** (2011) Discovery of large conical stromatolites in Lake Untersee, Antarctica. *Geobiology*, **9**, 280–293.

Ariztegui, D., Anselmetti, F.S., Gilli, A. and **Waldmann, N.** (2008) Late Pleistocene environmental changes in Patagonia and Tierra del Fuego – a limnogeological approach. In: *Developments in Quaternary Sciences Series 11* (Ed. J. Rabassa), The Late Cenozoic of Patagonia and Tierra del Fuego. ISBN 978-0-444-52954-1. Elsevier Science, pp. 430.

Arp, G., Reiner, A. and **Reitner, J.** (2003) Microbialite formation in seawater of increased alkalinity, satonda crater lake, Indonesia. *J. Sediment. Res.*, **73**, 105–127.

Arp, G., Helms, G., Karlinska, K., Schumann, G., Reimer, A., Reitner, J. and **Trichet, J.** (2012) Photosynthesis versus exopolymer degradation in the formation of microbialites on the atoll of Kiritimati, Republic of Kiribati, Central Pacific. *Geomicrobiol J.*, **29**, 29–65.

Awramik, S.M. and **Grey, K.** (2005) Stromatolites: biogenicity, biosignatures, and bioconfusion. *Proc. SPIE*, **5906**, 1–9.

Baumgartner, L.K., Reid, R.P., Dupraz, C., Decho, A.W., Buckley, D.H., Spear, J.R., Przekop, K.M. and **Visscher, P.T.** (2006) Sulfate reducing bacteria in microbial mats: changing paradigms, new discoveries. *Sed. Geol.*, **185**, 131–145.

Benzerara, K., Meibom, A., Gautier, Q., Kamierczak, J., Stolarski, J., Menguy, N. and **Brown, G.E.** (2010) Nanotextures of aragonite in stromatolites from the quasi-

marine Satonda crater lake, Indonesia. *Geochem. Soc. London Spec. Publ.*, **336**, 211–224.

Berner, R.A. (1975) The role of magnesium in the crystal growth of calcite and aragonite from sea water. *Geochim. Cosmochim. Acta*, **39**, 489–504.

Biller, S.J., Schubotz, F., Roggensack, S.E., Thompson, A.W., Summons, R.E. and **Chisholm, S.W.** (2014) Bacterial vesicles in marine ecosystems. *Science*, **343**, 183–186.

Bischoff, J.L. and **Fyfe, W.S.** (1968) Catalysis, inhibition, and the aragonite-calcite problem I. The aragonite-calcite transformation. *Am. J. Sci.*, **266**, 65–79.

Bradbury, J.P., Grosjean, M., Stine, S. and **Sylvestre, F.** (2001) Full and late glacial records along the PEP1 transect: their role in developing interhemispheric paleoclimate interactions. In: *Interhemispheric Climate Linkages* (Ed. V. Markgraf), pp. 265–292. Academic Press, San Diego, CA.

Burne, R.V. and **Moore, L.S.** (1987) Microbialites: organosedimentary deposits of benthic microbial communities. *Palaios*, **2**, 241–254.

Canfield, D.E. and **Des Marais, D.J.** (1991) Aerobic sulfate reduction in microbial mats. *Science*, **251**, 1471–1473.

Cartwright, A., Quade, J., Stine, S., Adams, K.D., Broecker, W. and **Cheng, H.** (2011) Chronostratigraphy and lake-level changes of Laguna Cari-Laufquén, Rio Negro, Argentina. *Quatern. Res.*, **76**, 430–440.

Casanova, J. and **Hillaire-Marcel, C.** (1993) Carbon and oxygen isotopes in African lacustrine stromatolites: palaeohydrological interpretation. In: *Climate Change in Continental Isotopic Record* (Ed. P.K. Swart), *Geophys. Monogr.*, **78**, 123–133.

Coira, B.L. (1979) Descripción geológica de la hoja 40 d Ingeniero Jacobacci. *Bol. Serv. Geol. Nac.*, **168**, 101.

Craig, H. and **Gordon, L.I.** (1965) Deuterium and oxygen 18 variations in the ocean and marine atmosphere. In: *Proc. Stable Isotopes in Oceanographic Studies and Paleotemperatures* (Ed. E. Tongiogi), pp. 9–130. V. Lishi e F., Pisa, Spoleto, Italy.

Craig, H., Dixon, F., Craig, V., Edmond, J. and **Coulter, G.** (1974) Lake Tanganyika geochemical and hydrographic study: 1973 expedition. *Scripps Inst. Oceanogr. Pub.*, **75**, 1–83.

Cusminsky, G., Schwalb, A., Pérez, A.P., Pineda, D., Viehberg, F., Whatley, R., Markgraf, V., Gilli, A., Ariztegui, D. and **Anselmetti, F.S.** (2011) Late Quaternary environmental changes in Patagonia as inferred from lacustrine fossil and extant ostracodes. *Biol. J. Linn. Soc.*, **103**, 397–408.

De Wit, R., Gautret, P., Bettarel, Y., Roques, C., Marlière, C., Ramonda, M., Nguyen Thanh, T., Tran Quang, H. and **Bouvier, T.** (2015) Viruses occur incorporated in biogenic high-Mg calcite from hypersaline microbial mats. *PLoS ONE*, **10**, e0130552.

Decho, A.W. (2000) Exopolymer microdomains as a structuring agent for heterogeneity within microbial biofilms. In: *Microbial Sediments* (Eds R.E. Riding and S.M. Awramik), pp. 1–9. Springer-Verlag, Berlin.

Decho, A.W. and **Kawaguchi, T.** (1999) Confocal imaging of natural in situ microbial communities and their extracellular polymeric secretions (EPS) using Nanoplast resin. *Biotechniques*, **27**, 1246–1251.

Del Valle, R.A., Tatur, A., Amos, A., Ariztegui, D., Bianchi, M.M., Cusminsky, G.C., Hsu, K., Lirio, J.M., Martínez Macchiavello, J.C., Masaferro, J.I., Núñez, H.J., Rinaldi, C.A., Valverde, R., Vigna, S., Vobis, G. and **Whatley, R.C.** (1993) Laguna Cari Laufquen Grande: registro de una fase climática húmeda del Pleistoceno tardío en la Patagonia septentrional. *Proyecto Pangea Glopals*, comunicaciones, San Juan, 16–19.

Del Valle, R.A., Lirio, J.M., Nuñez, H.J., Tatur, A., Rinaldi, C.A., Lusky, J.C. and **Amos, A.J.** (1996) Reconstrucción paleoambiental Pleistoceno-Holoceno en las latitudes medias al este de los Andes. *XIII Congr. Geol. Argent. III Congr. Expl. Hidrocarb Actas*, **IV**, 85–102.

Des Marais, D.J. (2003) Biogeochemistry of hypersaline microbial mats illustrates the dynamics of modern microbial ecosystems and the early evolution of the biosphere. *Biol. Bull.*, **204**, 160–167.

Desnues, C., Rodriguez-Brito, B., Rayhawk, S., Kelley, S., Tran, T., Haynes, M., Liu, H., Furlan, M., Wegley, L., Chau, B., Ruan, Y., Hall, D., Angly, F.E., Edwards, R.A., Li, L., Vega Thurber, R., Reid, P.R., Siefet, J., Souza, V., Valentine, D.L., Swan, B.K., Breitbart, M. and **Rohwer, F.** (2008) Biodiversity and biogeography of phages in modern stromatolites and thrombolites. *Nature*, **452**, 340–343.

Dupraz, C. and **Visscher, P.T.** (2005) Microbial lithification in marine stromatolites and hypersaline mats. *Trends Microbiol.*, **13**, 429–438.

Dupraz, C., Visscher, P.T., Baumgartner, L.K. and **Reid, R.P.** (2004) Microbe–mineral interactions: early carbonate precipitation in a hypersaline lake (Eleuthera Island, Bahamas). *Sedimentology*, **51**, 745–765.

Dupraz, C., Reid, R.P., Braissant, O., Decho, A.W., Norman, R.S. and **Visscher, P.T.** (2009) Process of carbonate precipitation in modern microbial mats. *Earth-Sci. Rev.*, **96**, 141–162.

Elser, J.J., Schampel, J.H., Garcia-Pichel, F., Wade, B.D., Souza, V., Eguiarte, L., Escalante, A. and **Farmer, J.D.** (2005) Effects of phosphorus enrichment and grazing snails on modern stromatolitic microbial communities. *Freshw. Biol.*, **50**, 1808–1825.

Farias, M.E., Rascovan, N., Toneatti, D.M., Albarracin, V.H., Flores, M.R., Poire, D.G., Collavino, M.M., Aguilar, M.O., Vazquez, M.P. and **Polerecky, L.** (2013) The Discovery of Stromatolites Developing at 3570 m above Sea Level in a High-Altitude Volcanic Lake Socompa, Argentinean Andes. *PLoS ONE*, **8**, e53497.

Forterre, P., Soler, N., Krupovic, M., Marguet, E. and **Ackermann, H.W.** (2013) Fake virus particles generated by fluorescence microscopy. *Trends Microbiol.*, **21**, 1–5.

Galloway, R.M., Markgraf, V. and **Bradbury, J.P.** (1988) Dating shorelines of lakes in Patagonia Argentina. *J. S. Am. Earth Sci.*, **1**, 195–198.

Glunk, C., Dupraz, C., Braissant, O., Gallagher, K.L., Verrecchia, E.P. and **Visscher, P.T.** (2011) Microbially mediated carbonate precipitation in a hypersaline lake, Big Pond (Eleuthera, Bahamas). *Sedimentology*, **58**, 720–738.

González Bonorino, F. and **Rabassa, J.** (1973) La laguna Cari-laufquen Grande y el origen de los bajos patagónicos. *Rev. Asoc. Geol. Argent. Rev.*, **28**, 314–318.

Grilli Caiola, M., Ocampo-Friedmann, R. and **Friedmann, E.I.** (1993) Cytology of long-term desiccation in the desert cyanobacterium *Chroococcidiopsis* (Chroococcales). *Phycologia*, **32**, 315–322.

Grotzinger, J.P. and **Rothman, D.H.** (1996) An abiotic model for stromatolite morphogenesis. *Nature*, **383**, 423–425.

Hofmann, H.J., Grey, K., Hickman, A.H. and **Thorpe, R.I.** (1999) Origin of 3.45 Ga coniform stromatolites inWarrawoona Group, Western Australia. *Geol. Soc. Amer. Bull.*, **111**, 1256–1262.

Logan, B.W. and **Cebulski, D.E.** (1970) Sedimentary environments of Shark Bay, Western Australia. In: *Carbonate Sedimentation and Environments, Shark Bay, Western Australia*, Vol. 13 (Eds B.W. Logan, G.R. Davies, J.F. Read and D.E. Cebulski), pp. 1–37. American Association of Petroleum Geologists, Tulsa, OK.

McLoughlin, N., Wilson, A. and **Brasier, M.D.** (2008) Growth of synthetic stromatolites and wrinkle structures in the absence of microbes – implications for the early fossil record. *Geobiology*, **6**, 95–105.

Meyer, H., Schönicke, L., Wand, U., Hubberten, H.-W. and **Friedrichsen, H.** (2000) Isotope studies of hydrogen and oxygen in ground ice – experiences with the equilibration technique. *Isot. Environ. Health Stud.*, **36**, 133–149.

Müller, G., Irion, G. and **Forstner, U.** (1972) Formation and diagenesis of inorganic Ca-Mg carbonates in the lacustrine environment. *Naturwissenschaften*, **59**, 158–164.

Pacton, M., Gorin, G.E. and **Vasconcelos, C.** (2011) Amorphous organic matter – experimental data on formation and the role of microbes. *Rev. Palaeobot. Palynol.*, **166**, 253–267.

Pacton, M., Ariztegui, D., Wacey, D., Kilburn, M.R., Rollion-Bard, C., Farah, R. and **Vasconcelos, C.** (2012) Going nano: a new step toward understanding the processes governing freshwater ooid formation. *Geology*, **40**, 547–550.

Pacton, M., Wacey, D., Corinaldesi, C., Tangherlini, M., Kilburn, M.R., Gorin, G., Danovaro, R. and **Vasconcelos, C.** (2014) Viruses as a new agent of organomineralisation in the geological record. *Nat. Commun.*, **5**, 4298.

Petryshyn, V.A., Corsetti, F.A., Berelson, W.M., Beaumont, W. and **Lund, S.P.** (2012) Stromatolite lamination frequency, Walter Lake, Nevada: implications for stromatolites as biosignatures. *Geology*, **40**, 499–502.

Plée, K., Ariztegui, D., Martini, R. and **Davaud, E.** (2008) Unravelling the microbial role in ooids formation – results of an in situ experiment in modern freshwater Lake Geneva in Switzerland. *Geobiology*, **6**, 341–360.

Reid, R.P., Visscher, P.T., Decho, A.W., Stolz, J.F., Bebout, B.M., Dupraz, C., Macintyre, L.G., Paerl, H.W., Pinckney, J.L., Prufert-Bebout, L., Steppe, T.F. and **Des Marais, D.J.** (2000) The role of microbes in accretion, lamination and early lithification of modern marine stromatolites. *Nature*, **406**, 989–992.

Riding, R.E. (2011) Microbialites, stromatolites and thrombolites. In: *Encyclopedia of Geobiology* (Eds J. Reitner and V. Thiel), pp. 635–654. Encyclopedia of Earth Science Series. Springer, Heidelberg.

Schwalb, A., Burns, S., Cusminsky, G., Kelts, K. and **Markgraf, V.** (2002) Assemblage diversity and isotopic signals of modern ostracodes and host waters from Patagonia, Argentina. *Palaeogeogr. Palaeoclimatol. Palaeoecol.*, **187**, 323–339.

Solari, M.A., Hervé, F., Le Roux, J.P., Airo, A. and **Sial, A.N.** (2010) Paleoclimatic significance of lacustrine microbialites: a stable isotope case study of two lakes at Torres del Paine, southern Chile. *Palaeogeogr. Palaeoclimatol. Palaeoecol.*, **297**, 70–82.

Soler, N., Krupovic, M., Marguet, E. and **Forterre, P.** (2015) Membrane vesicles in natural environments: a major challenge in viral ecology. *ISME J.*, **9**, 793–796.

Souza-Egipsy, V., Wierzchos, J., Ascaso, C. and **Nealson, K.H.** (2005) Mg-silica precipitation in fossilization mechanisms of sand tufa endolithic microbial community, Mono Lake (California). *Chem. Geol.*, **217**, 77–87.

Stolz, J.F. (1991) *Structure of Phototrophic Prokaryotes*. CRC Press, Boca Raton, 131 pp.

Stolz, J.F., Feinstein, T.N., Salsi, J., Visccher, P.T. and **Reid, R.P.** (2001) TEM analysis of microbial mediated sedimentation and lithification in a modern marine stromatolite. *Am. Mineral.*, **86**, 826–833.

Suttle, C.A. (2005) Viruses in the sea. *Nature*, **437**, 356–361.

Tatur, A., del Valle, R., Bianchi, M.M., Outes, V. and **Villarosa, G.** (2000) Late Pleistocene Pluvial Phase in Patagonia. *Geolines*, **11**, 47–51.

Trichet, J. and **Défarge, C.** (1995) Non-biologically supported organo mineralization. In: *Bulletin de l'Institut Océanographique de Monaco* (Eds D. Allemand and J.P. Cuif), *Proc. 7th Int. Symp. Biomineral.*, **2** (14>), 203–236.

Valero-Garcés, B.L., Arenas, C. and **Delgado-Huertas, A.** (2001) Depositional environments of Quaternary lacustrine travertines and stromatolites from high-altitude Andean lakes, northwestern Argentina. *Can. J. Earth Sci.*, **38**, 1263–1283.

Visscher, P.T., Reid, R.P. and **Bebout, B.M.** (2000) Microscale observations of sulfate reduction: correlation of microbial activity with lithified micritic laminae in modern marine stromatolites. *Geology*, **28**, 919–922.

Volkheimer, W. (1973) Observaciones geológicas en el área de Ingeniero Jacobacci y adyascencias (provincia de Río Negro). *Rev. Asoc. Geol. Arg.*, **28**, 13–36.

Whatley, R. and **Cuminsky, G.** (1999) Lacustrine Ostracoda and late Quaternary palaeoenvironments from the Lake Cari-Laufquen region, Rio Negro province, Argentina. *Palaeogeogr. Palaeoclimatol. Palaeoecol.*, **151**, 229–239.

Wright, P.V. (2012) Lacustrine carbonates in rift settings: the interaction of volcanic and microbial processes on carbonate deposition. In: *Advances in Carbonate Exploration and Reservoir Analysis* (Eds J. Garland, J.E. Neilson, S.E. Laubach and K.J. Whidden), *Geol. Soc. London. Spec. Publ.*, **370**. doi: 10.1144/SP370.2.

